Preprint Title	Phenanthridine-pyrene conjugates as fluorescent probes for DNA/RNA and an inactive mutant of dipeptidyl peptidase enzyme
Authors	Josipa Matić, Tana Tandarić, Marijana Radić Stojković, Filip Šupljika, Robert Vianello and Lidija-Marija Tumir
Publication Date	02 Jan. 2023
Article Type	Full Research Paper
Supporting Information File 1	ESI Matić et all.docx; 1.9 MB
ORCID® iDs	Josipa Matić - https://orcid.org/0000-0003-1774-0446; Marijana Radić Stojković - https://orcid.org/0000-0003-4040-6534; Lidija-Marija Tumir - https://orcid.org/0000-0002-8400-2622

Phenanthridine-pyrene conjugates as fluorescent probes for DNA/RNA and an inactive mutant of dipeptidyl peptidase enzyme

Josipa Matić[a], Tana Tandarić[b], Marijana Radić Stojković[a], Filip Šupljika[c], Robert Vianello, [b]* Lidija-Marija Tumir [a]*

[a]Laboratory for Biomolecular Interactions and Spectroscopy, Division of Organic Chemistry and Biochemistry, Ruđer Bošković Institute, Bijenička cesta 54, 10000 Zagreb, Croatia, E-mail: tumir@irb.hr

[b]Laboratory for the Computational Design and Synthesis of Functional Materials, Division of Organic Chemistry and Biochemistry, Ruđer Bošković Institute, Bijenička cesta 54, 10000 Zagreb, Croatia, E-mail: robert.vianello@irb.hr

[c]Laboratory for Physical Chemistry and Corrosion, Department of Chemistry and Biochemistry, Faculty of Food Technology and Biotechnology, University of Zagreb, Croatia

*Corresponding author

Abstract

Two novel hybrid molecules were designed: pyrene and phenanthridine-amino acid units with a different linker length between aromatic fragments. Molecular modelling combined with spectrophotometric experiments revealed that in neutral and acidic buffered water solutions conjugates predominantly exist in intramolecularly stacked conformations because of the π-π stacking interaction between pyrene and phenanthridine moieties. Investigated systems exhibited pH-dependent excimer formation that is significantly red-shifted relative to the pyrene and phenanthridine fluorescence. While conjugate with a short linker showed negligible spectrophotometric changes due to the polynucleotide addition, conjugate with longer and more flexible linker exhibited a micro-molar and sub-micro-molar binding affinity for ds-polynucleotides and inactive mutant of dipeptidyl peptidase enzyme E451A.

Keywords

Dipeptidyl peptidase enzyme; excimer; phenanthridine; polynucleotide; pyrene

Introduction

The design of small molecules that are able to selectively bind and discriminate different biomolecular structures (polynucleotides vs proteins, DNA or RNA, single or double stranded polynucleotides, particular base composition…) and signalize binding by specific spectroscopic response is of great importance [1-2].

Pyrene derivatives are among the earliest known fluorescent probes for biomolecules. These chromophores are often used due to their high extinction coefficient and long emission lifetime (>100 ns) [3]. Their large aromatic hydrophobic surface allows the intercalation between DNA/RNA base

pairs and binding within minor groove. Pyrenes are also prominent protein probes that can monitor protein conformational changes because of pyrene sensitivity to the polarity of its surroundings. Similar as pyrenes, phenanthridines are also used as fluorescent probes whose properties could be modified by different substituents attached to the aromatic core. It is known that two or more pyrenes form an excimer [4], where fluorescence band of single pyrene molecule is significantly shifted to longer wavelengths upon inter- or intramolecular stacking of pyrene moieties. Phenanthridine derivatives were extensively investigated in our group and previous studies have shown that two phenanthridine units can also form an excimer, characterized by a specific fluorescence band [5-6].
Some of the compounds from both described classes, pyrenes and phenanthridines, showed significant biological activity. It has been reported that some pyrene-guanidiniocarbonyl pyrrole derivatives exhibited strong pH-dependent affinity towards ds-DNA which could be modified by the flexibility of the linker connecting those two units [7]. Further, pyrene-guanidiniocarbonyl-pyrrole discriminated DNA and RNA by different spectroscopic (namely, induced circular dichroism signal and fluorescent signal) response [8]. Also, we recently reported pyrene–quinoline hybrid molecule that formed exciplex [9], as well as conjugates formed of pyrene and amino acid-fluorescent nucleobase derivative qAN1, differing in length and flexibility between fluorophores [10]. Both conjugates strongly interacted with ds-DNA/RNA grooves with similar affinity but opposite fluorescence response, due to pre-organization. Compounds that consisted of pyrrole guanidine attached to larger aryl moieties (pyrene and phenanthridine) bind to the human DPP III enzyme [11]. Pyrene-cyanine hybrids connected with rigid triazole-peptide linker were designed and synthesized in our group and showed strong pyrene emission change upon binding to proteins, and cyanine fluorescence that was selective for polynucleotides. Moreover, FRET pair of chromophores was activated upon binding to biomolecules [12].

As a continuation of our previous work, two phenanthridine-pyrene conjugates **Phen-Py-1** and **Phen-Py-2** (Scheme 1), differing only in the linker length between aromatic units, have been prepared by condensation of two different pyrene-carboxylic acids with phenanthridine-labelled amino acid (Scheme 1).

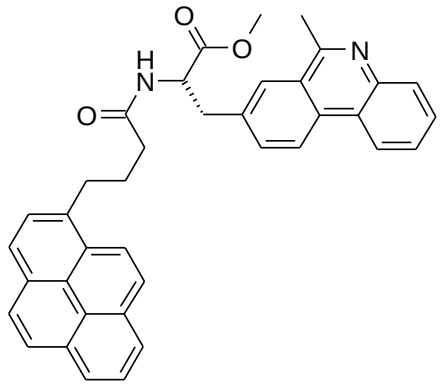

Phen-Py-1

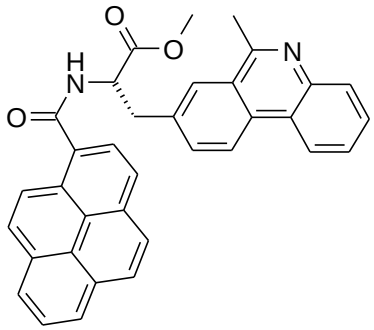

Phen-Py-2

Scheme 1. Novel pyrene-phenanthridine conjugates **Phen-Py-1** (longer, flexible linker) and **Phen-Py-2** (shorter, rigid linker)

New conjugates **Phen-Py-1** and **Phen-Py-2** exhibited excimer formation and showed new fluorescence emission bands at 495 nm and 485 nm, respectively, which were significantly red-shifted compared to the fluorescence of either single phenanthridine or pyrene molecules. Excimer fluorescence of **Phen-Py-1** was pH-dependent: excimer band was quenched with a decrease of pH value. To the best of our knowledge, these were the first reported phenanthridine-pyrene excimers. To

gain a better understanding of these complexes and interpret their conformational preference in solution, we have conducted molecular dynamics simulations, which showed similar degree of intramolecular stacking of phenanthridine and pyrene in buffered water solution for both **Phen-Py-1** and **Phen-Py-2**. However, the two compounds revealed different fluorimetric response upon polynucleotides binding. Also, compound **Phen-Py-1** bound to human dipeptidyl peptidase III enzyme with a micromolar affinity which can be monitored by a significant change in the fluorescence spectra of the compound.

Results and discussion

Synthesis

Phenanthridine derivative of alanine amino acid (**Phen-AA**) has been prepared according to the procedure described earlier [13]. **Phen-AA** was deprotected in acidic conditions (TFA-H_2O) and coupled with pyrene-carboxylic acid in the presence of triethylamine (TEA) *N*,*N*,*N'*,*N'*-tetramethyl-*O*-(1*H*-benzotriazol-1-yl)uronium hexafluorophosphate (HBTU) as the coupling reagent, and 1-hydroxybenzotriazole (HOBT) as a coupling additive to give products **Phen-Py-1** and **Phen-Py-2** (Scheme 2).

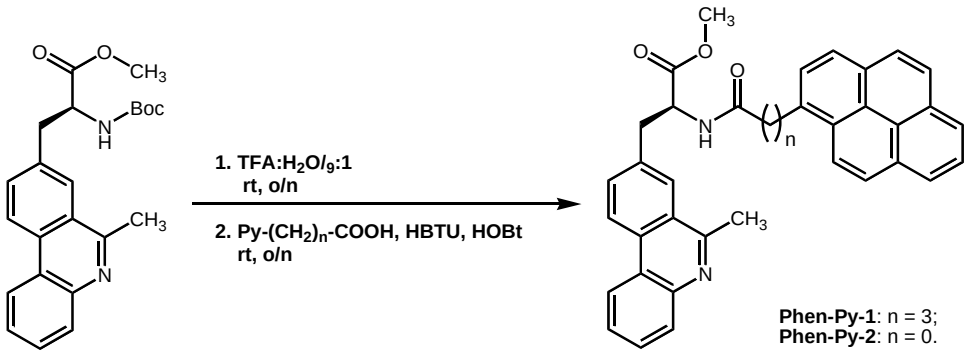

Scheme 2. Synthesis of products **Phen-Py-1** and **Phen-Py-2** by peptide coupling reaction; Reagents and conditions: 1. TFA-H_2O mixture (9:1, v/v; 2 mL), r.t. overnight; 2. Dry acetonitrile, HBTU, HOBt, Et_3N, r.t., overnight

Spectroscopic characterization of Phen-Py-1-2 in the aqueous solution

UV-Vis spectra

Studied compounds **Phen-Py-1-2** were moderately soluble in DMSO (up to $c = 1 \times 10^{-3}$ mol dm^{-3}) and their stock solutions were stable during few months. All measurements were recorded in the Na-cacodylate buffer (I_c= 0.05 mol dm^{-3}) both at pH = 5.0 and pH = 7.0 for comparison, since phenanthridine heterocyclic nitrogen becomes protonated in weakly acidic conditions (pH = 5) [14-15]. Volume ratio of DMSO was less than 1% in all measurements. Absorbencies of aqueous solutions f compounds **Phen-Py-1** and **Phen-Py-2** were proportional to their concentrations up to $c = 3 \times 10^{-6}$ mol dm^{-3}. Deviation of Lamberts-Beer law, decrease of UV-Vis spectra upon heating up to 90 °C and baseline increase indicated intermolecular stacking and aggregation of compounds that was more pronounced for **Phen-Py-2**. Spectroscopic characterization was given in the ESI (Table S1 and Fig. S1).

Intramolecular contacts between phenanthridine and pyrene chromophore was enabled by a linker between chromophores. This stacking interaction minimized surface area that was exposed to water. As a result, mutual shielding of chromophores and coulombic interaction between induced dipoles could cause hypochromism and consequent decrease of ε value [16-18], although this decrease was not an accurate measure of the shielding degree [19-21].
In order to determine the hypochromic effect (% H) at single wavelength, UV-Vis absorption of examined compounds was compared with the absorption of referent compounds (Scheme S2, ESI†) that possessed the same chromophores. Therefore, UV-Vis absorption of **Phen-Py-1-2** was compared with the sum of the absorption of **Phen-AA** [5, 13] (comprising phenanthridine unit, Scheme S2, ESI†) and the absorption of 1-pyrenebutyric acid **PBA** (containing pyrene unit, Scheme S2, ESI†). Noticeable hypochromic effect (% H) was observed for both **Phen-Py-1-2.** Hypochromic effect was stronger at pH = 5 (55% and 53% for **Phen-Py-1** and **Phen-Py-2**, respectively) than at pH = 7 (35% and 48% for **Phen-Py-1** and **Phen-Py-2**, respectively). Phenanthridine nitrogen was protonated at weakly acidic condition, which made the phenanthridinium moiety relatively electron deficient compared to electron rich pyrene moiety that favored intramolecular stacking. The pronounced hypochromic effect, was additionally supported by molecular dynamics simulations. (Chapter **Computational analysis**).

Fluorescence spectra

Fluorescence emission of **Phen-Py-1-2** measured at pH = 5 and pH = 7 (cacodylate buffer, I_c =0.05 mol dm^{-3}) was linearly dependent on the concentration up to 3×10^{-6} mol dm^{-3}. Excitation spectra of conjugates **Phen-Py-1-2** were in good agreement with their UV-Vis spectra. Phenanthridine-pyrene conjugate **Phen-Py-1** exhibited excimer formation characterized by new fluorescence emission band at 475 nm, which is significantly red-shifted compared to either fluorescent emission of single phenanthridine (λ_{max} = 400 nm) or pyrene (λ_{max} = 378 and 400 nm) molecule (Figure S2, left pH = 5.0; right pH = 7.0, ESI). **Phen-Py-2** also showed shoulder at 480 nm (besides main emission signal at 400 nm) that could be attributed to the excimer formation (Figure S2, ESI). For **Phen-Py-1**, the excimer formation was observed both upon excitation at 280 nm and 350 nm and it was found to be pH-dependent (Figure 1). Further, excimer signal was observed in water, but not in methanol (Figure S3, ESI), due a to lower dielectric constant and a lower polarity that influenced intramolecular stacking. To the best of our knowledge, these is the first reported phenanthridine-pyrene excimer.

Molecular dynamics calculations (see Chapter **Computational analysis**) and hypochromism observed from UV-Vis spectra pointed towards stronger intramolecular stacking interactions at weakly acidic condition (pH = 5.0) compared to pH = 7 for both compounds. Also, pyrene-phenanthridine π-overlap was more pronounced for **Phen-Py-2**. On the other hand, excimer signal (475 nm) of **Phen-Py-1** was significantly stronger at weakly basic and neutral conditions at which intramolecular stacking was less pronounced. At acidic conditions, monomer signal (400 nm) was dominant (Figure 1).

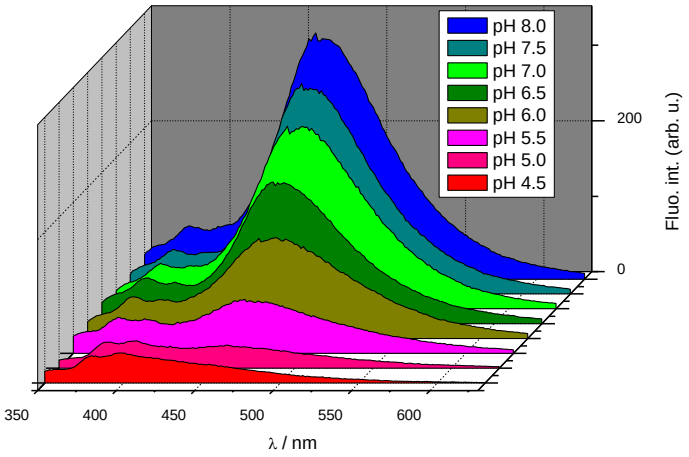

Figure 1. Fluorescence emission spectra of **Phen-Py-1** (c = 2 × 10^{-6} mol dm^{-3}) at different pH values (Na-cacodylate, HCl, I_c = 0.05 mol dm^{-3} at 25 °C (λ_{exc} = 280 nm).

Emission of excimer did not exclusively depend on the degree of overlapping of chromophores, although this stacking was necessary for FRET (Förster resonance energy transfer). Earlier theoretical examinations favored symmetrical sandwich configuration as optimal for the largest exciton splitting, while other reports suggested favored orientation with one aromatic moiety displaced (ca 1.4 Å) from the other to minimize van der Waals repulsion [22]. Obviously, redistribution of charges at acidic pH (protonated phenanthridine nitrogen) compared to neutral pH (unprotonated phenanthridine nitrogen) caused more efficient stacking and hypochromic effect. However, the energy transfer between chromophores and resulting excimer fluorescence was increased at neutral and basic condition. Excimer fluorescence was obviously sensitive to small changes in mutual orientation of chromophores. Another possible explanation of excimer fluorescence is the formation of intermolecular complexes which were responsible for the excimer emission and were more favorable at neutral pH. To explore these hypotheses, detailed spectroscopic measurements would have to be carried out, which were outside of the scope of the current work.

Computational analysis

In order to examine conformational features of **Phen-Py-1–2**, and inspect whether their intrinsic dynamics in aqueous solution play a role in determining their ability to form stacked aggregates and excimers, we performed molecular dynamics (MD) simulations of different protonation forms of **Phen-Py-1–2** placed in the explicit water solvation, and analyzed structural preferences in the obtained trajectories.

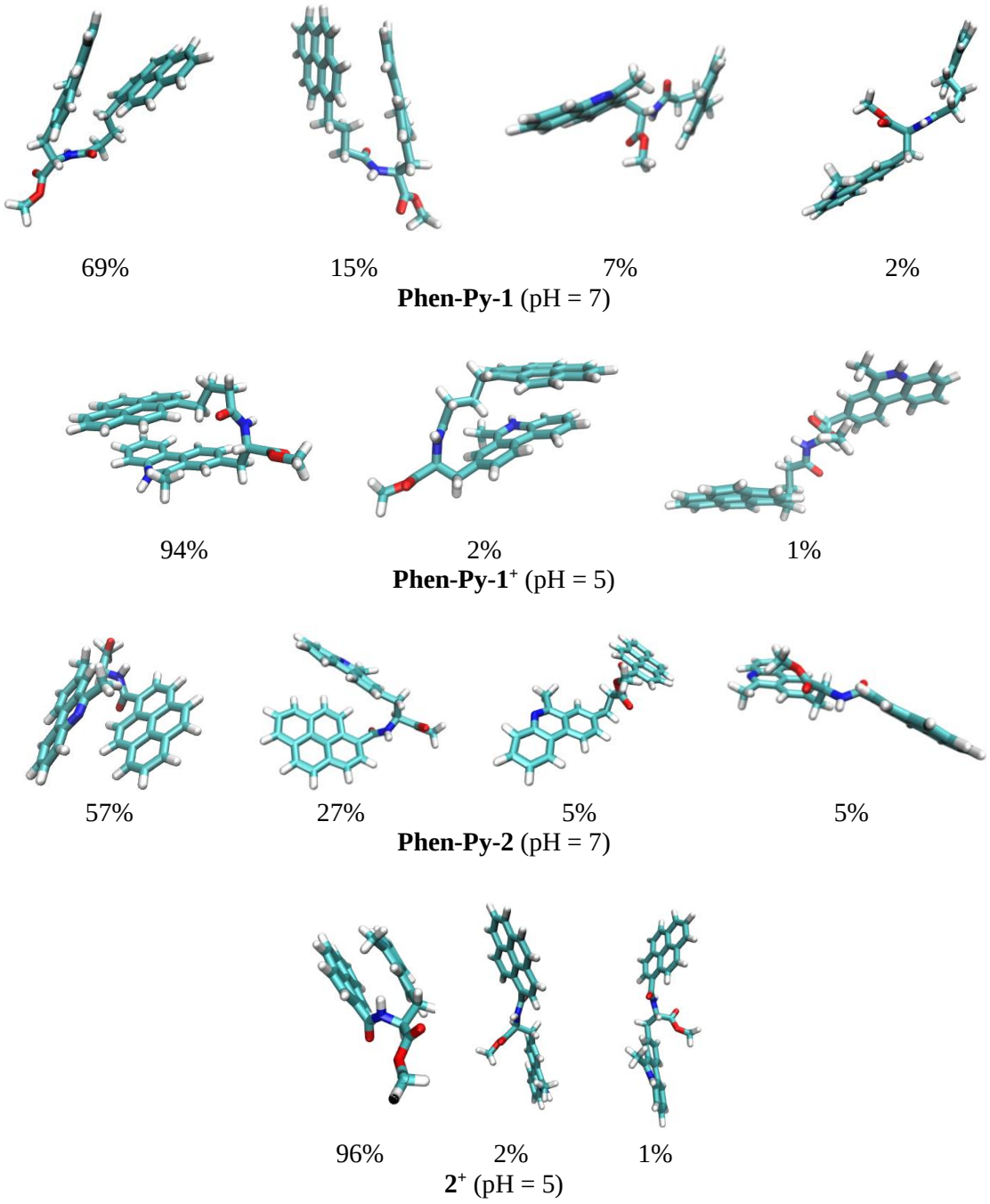

Figure 2. Most representative structures of conjugates **Phen-Py-1**–**2** at different pH conditions and their overall populations during MD simulations. These were identified after the clustering analysis of the corresponding MD trajectories.

In setting up our simulations, we prepared the geometries of unionized **Phen-Py-1**–**2** and their monocations, protonated at the phenanthridine nitrogen atom. These structures correspond to pH values of pH = 7 and pH = 5, respectively, in accordance with experiments conducted here. Taking the experimental pK_a value of the isolated phenanthridine, pK_a = 4,65 [23] our calculated pK_a of methyl-phenanthridine is pK_a = 6.3. We assumed that this value will not change much in the prepared conjugates, which confirms that both **Phen-Py-1**–**2** are monoprotonated at pH = 5. We submitted all four systems to molecular dynamics simulations and performed clustering analysis on the obtained

structures. The most representative geometries that account for the majority of the population of each system are presented in Figure 2.

The results showed that both conjugates, irrespective of their protonation state, prefer stacked conformations, with favorable π–π interactions among aromatic fragments. Interestingly, this also holds even for a formally more rigid **Phen-Py-2**, as it turned out that the ethyl chain possesses enough flexibility to enable the intramolecular contacts. Still, one observes that folded structures are more frequent in monoprotonated derivatives **Phen-Py-1**$^+$ and **Phen-Py-2**$^+$, where the stacking π–π interactions are further promoted by favorable cation–π interactions. In other words, in **Phen-Py-1**$^+$ and **Phen-Py-2**$^+$, stacked structures account for around 96% and 98% of population, respectively, while in unionized **Phen-Py-1** and **Phen-Py-2** these cluster around 84% in both cases (Figure 2). This is further supported by inspecting the evolution of distances between the centers of mass among aromatic units (Figure S22), which are found around 5.5 Å for both conjugates under acidic conditions, at the same time exceeding 8 Å (**Phen-Py-1**) and 6 Å (**Phen-Py-2**) under neutral conditions. All of this convincingly indicates that monoprotonated analogues are less available for both the intermolecular interactions among systems in solution and the subsequent formation of intermolecular excimers.

Further, although interaction of pyrene and phenanthridine is necessary for FRET, it seems that higher degree of aromatic surfaces overlapping and cation–π interactions also yield excimer fluorescence quenching [22, 24-25]. This conclusion is strongly in line with experimental insight reported here and helps in explaining the observed excimer fluorescence quenching with a decrease in the solution pH value as well as with the stronger excimer fluorescence of **Phen-Py-1** compared to **Phen-Py-2.**

In order to check the validity of the premise that systems **Phen-Py-1**–**2** are well represented in the aqueous solution with the most dominant structures given in Figure 2, we calculated energies of the excited states responsible for the experimental UV/Vis spectra in Figure S23 corresponding to isolated conjugates. For that purpose, we used the most abundant structure of each system in Figure 2 and performed the geometry optimization by the M06-2X/6–31+G(d) approach with solvent effects modelled through the IEF-PCM implicit water solvation, followed by the TD-DFT computations at the same level of theory. The obtained vertical transitions corresponding to absorption maxima at pH = 7.0 are 260 and 372 nm (**Phen-Py-1**), and 270 and 397 nm (**Phen-Py-2**), while at pH = 5.0 are 265 and 357 nm (**Phen-Py-1**$^+$), and 266 and 366 nm (**Phen-Py-2**$^+$). These are found in very good agreement with experimental results presented in Table S1, which lends credence to the computational approach utilized here and confirms the validity of the clustering analysis. This conclusion is further strengthened by the fact that the same approach gave the absorption maximum of 256 nm for the isolated phenanthridine at pH = 7.0, which is in excellent agreement with the experimental value of 248 nm, [26] and well matched with 250 nm reported here for Phen-AA (Table S1)

Interactions of Phen-Py-1-2 with *ds*-polynucleotides and enzyme dipeptidyl peptidase III in an aqueous medium

Hybrid compounds **Phen-Py-1-2** were examined for DNA/RNA binding affinity and eventual preference for different polynucleotide structures. For example, B-helical structure had well-defined minor groove that was suitable for minor groove binding, while A-helical structure was favorable for intercalation and/or major groove binding. *Calf thymus* DNA (*ct*-DNA, 58% AT and 42% GC base pairs) and poly rA – poly rU (RNA) were chosen as models for a classical B-helical and A-helical structure, respectively [27]. Unlike **Phen-Py-2**, compound **Phen-Py-1** showed notable spectroscopic response upon binding, thus additional experiments of **Phen-Py-1** with synthetic DNA polynucleotides [17], poly(dAdT)$_2$ and poly(dGdC)$_2$ and enzyme dipeptidyl peptidase III (E451, inactive DPP III mutant) were performed.

Interactions of **Phen-Py-1-2** with DNA and RNA were studied by fluorimetric titrations, thermal melting experiments, and CD titrations. Excimer bands showed photobleaching, therefore for the purpose of spectrophotometric titrations, buffered solutions of compounds were prepared 24 hours before, to ensure stabile compound spectra. Fluorimetric titrations of both compounds with DNA/RNA showed only negligible and/or linear fluorescence change at weakly acidic condition (protonated form of hybrid molecule, pH = 5, Figure S7-S10, ESI). Further, **Phen-Py-2** showed negligible and/or linear fluorescence change upon addition of *ct*-DNA also at pH = 7 (Figure S11-S12, ESI).), while for **Phen-Py-1**, more notable fluorescence changes at pH 7 (neutral form) were observed. Thus, all further studies were performed at pH = 7.

Thermal melting studies

Binding of small molecule to double stranded DNA or RNA polynucleotides usually affect stability of double helix. This stabilization or destabilization revealed as change of polynucleotide's melting temperature ΔT_m value that was difference of the T_m value of free polynucleotide and T_m value of polynucleotide-small molecule complex.[28] Thermal melting experiments showed that hybrid molecules **Phen-Py-1-2** had only negligible effect on double helix stability (below 0.5 °C), both for DNA and RNA (Table S2, Figures S4–S6, ESI).

Spectrophotometric titrations

Excimer fluorescence signal of **Phen-Py-1** (longer linker between phenanthridine and pyrene unit) at 470 nm was quenched up to 30% upon addition of polynucleotides combined with significant hypsochromic (blue) shift of emission maxima (10-20 nm). Similar fluorimetric response with respect to excimer band was obtained independently on polynucleotide's structure and/or base composition. Monomer fluorescence emission at 400 nm was not changed except for titration with poly dGdC - poly dGdC where small increase of emission at 400 nm was observed. At ratios of an excess of polynucleotide over compound ($r_{[compound]\ /\ [polynucleotide]}$ <0.3) spectral changes could be attributed to single dominant binding mode. Titration data were processed by Scatchard equation [29-30] and Global Fit procedure [31] to calculate association constants and ratio $n_{[bound\ compound]\ /\ [polynucleotide]}$ (Figure 3, Figures S13-S16, Table S3). Compound **Phen-Py-1** showed high, micromolar/submicromolar affinities for all examined polynucleotides.

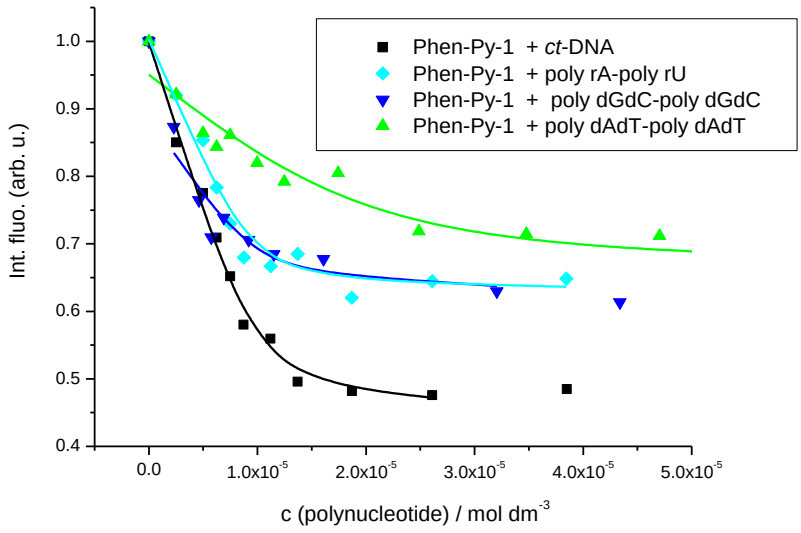

Figure 3. Experimental (■) and calculated (–) (by Scatchard eq., Table 1) fluorescence intensities of compounds **Phen-Py-1** upon addition of different ds-polynucleotides; fluorescence intensities were normalized for easier comparison. Na-cacodylate buffer, pH 7.0, I_c = 0.05 mol dm^{-3}, λ_{exc} = 352 nm, λ_{em} = 471 nm.

Binding of **Phen-Py-1** to polynucleotides likely leads to the unstacking of intramolecular pyrene-phenanthridine dimer and consequent excimer fluorescence quenching. Concurrently, no monomer fluorescence signal at 400 nm changed, except a small increase upon poly dGdC - poly dGdC addition. Negligible thermal stabilization (Table S2, Figures S4–S6†) did not support classical intercalation of phenanthridine and/or pyrene moiety, but there was a possibility of partial intercalation of pyrene or phenanthridine or even both aromatic units. Based on fluorescence response it was hard to discriminate extent of binding contribution of phenanthridine or pyrene moiety, although the presented computational analysis would support the binding of intramolecularly stacked dye in the polynucleotide groove or unspecific binding of stacked dye along the polynucleotide backbone as alternative possibility. Quenching of excimer fluorescence could be explained by reorganized intramolecular conformation of ligand and/or redistribution of chromophore charges upon binding, since fluorescence quenching is sensitive to factors that affect the rate and probability of contact, including steric shielding and charge-charge interactions [32].

Binding of **Phen-Py-1** to dipeptidyl peptidase (DPPIII) inactive enzyme mutant E451A was also examined by fluorimetric titrations, and it was found **Phen-Py-1** binds to the protein with a submicromolar affinity (log K_s = 7.54, n = 1; Table S3. ESI). This protein is a mono-zinc metalloexopeptidase and hydrolyses dipeptides from the N-termini of substrates that are consisting of at least tree amino acids. DPPIII participates in intracellular protein catabolism, has a function in pain modulation and oxidative stress. These biological functions make DPPIII a valuable target for the drug development. Interestingly, although excimer emission was totally quenched, emission of pyrene monomer was increased upon addition of enzyme (Figure 4), suggesting important role of hydrophobic pyrene subunit for protein binding [12].

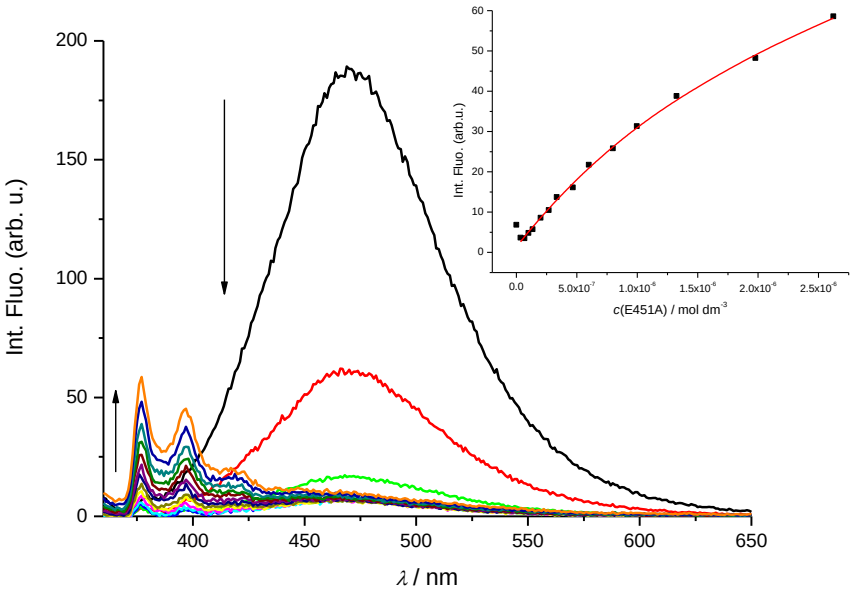

Figure 4. Fluorimetric titration of **Phen-Py-1**, λ_{exc} = 352 nm, c = 1 × 10^{-6} mol dm^{-3} with dipeptidyl peptidase (DPPIII) enzyme mutant E451A, Inset: Experimental (●) and calculated (—) fluorescence intensities of **Phen-Py-1** at λ_{em} = 377 nm upon addition of dipeptidyl peptidase (DPPIII) enzyme mutant E451A (pH = 7.4, Tris-HCl buffer, I_c = 0.02 mol dm^{-3}).

Circular dichroism (CD) experiments

CD spectroscopy was chosen to monitor conformational changes of polynucleotide's secondary structure induced by small molecule binding [33]. Compounds **Phen-Py-1** and **Phen-Py-2** were built using chiral amino acid building blocks and consequently had intrinsic CD spectrum. While changes of poly rA-poly rU spectra upon titration with **Phen-Py-1** and **Phen-Py-2** were negligible (Figure S18-S19, ESI), addition of **Phen-Py-1-2** to the *ct*-DNA caused change of signal at 270 nm (Figure S17, ESI) and at wavelengths longer than 300 nm. Intrinsic spectra of compound also had to be taken into account. Hence sum of ct-DNA and **Phen-Py-1** or **Phen-Py-2** CD spectra was compared to CD spectra of DNA-dye complex at the same concentration (Figure 5).

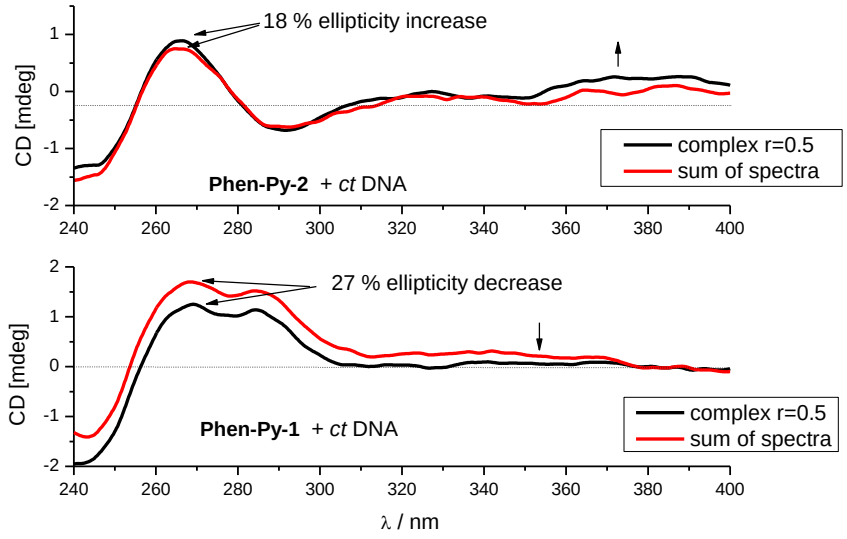

Figure 5. Comparison of spectra of DNA-dye complex (r = 0.5, —) and sum of DNA and dye spectra (—) of appropriate concentrations (c (*ct*-DNA) = 2 × 10^{-5} mol dm^{-3}, c (dye) = 1 × 10^{-5} mol dm^{-3}, Na-cacodylate buffer, pH = 7.0, I_c = 0.05 mol dm^{-3}).

Interestingly, complex of **Phen-Py-1**-*ct*-DNA showed decrease of CD signal compared to sum of **Phen-Py-1** and *ct*-DNA spectra, while complex of **Phen-Py-2**-*ct*-DNA showed small increase of CD spectra compared to sum of **Phen-Py-2** and *ct*-DNA. It was important to note that besides existence of dyes intrinsic spectra, UV absorption area of examined dyes (both phenanthridine and pyrene moiety) partly overlapped with the area of DNA/RNA absorption. Therefore it was difficult to distinguish if the changes in the 240-290 nm region were caused by a distortion of polynucleotide helicity upon addition of **Phen-Py-1**, or this change was result of uniform orientation of dye with respect to DNA chiral axis. Further, small decrease of CD signal in the pyrene absorption region (wavelengths longer than 300 nm) suggested possibility of partial intercalation of pyrene unit between base pairs. Similarly, small increase upon addition of **Phen-Py-2,** especially in the region >300 nm could be a consequence of groove binding of intramolecularly stacked compound **Phen-Py-2**.

Conclusions

Two novel phenanthridine-pyrene conjugates **Phen-Py-1-2** were prepared by the condensation of phenanthridinyl-alanine with the corresponding pyrene-containing carboxylic acid, and were linked together by an amide bond. Conjugate **Phen-Py-1** possessed tri-methylene chain linker that allowed a pronounced flexibility for positioning of aromatic units. Although more rigid, **Phen-Py-2** also enabled intramolecular stacking interaction between phenanthridine and pyrene. UV-Vis spectra of **Phen-Py-1-2** showed hypochromic effect at single wavelength compared to referent compounds with identical chromophores. This noticeable hypochromicity was the consequence of the intramolecular stacking upon the aromatic interaction between phenanthridine and pyrene, which was more pronounced at weakly acidic pH where the phenanthridine nitrogen was protonated. Experimental data were in good agreement with molecular dynamics simulations, which confirmed that folded structures are more frequent in monoprotonated derivatives **Phen-Py-1**$^+$ and **Phen-Py-2**$^+$, where π–π stacking contacts are further promoted by the favorable cation–π interactions.

Phenanthridine-pyrene conjugates **Phen-Py-1** showed excimer fluorescence that was red shifted compared to emission of single phenanthridine or pyrene chromophore. This excimer fluorescence was significantly solvent and pH dependent. Namely, excimer fluorescence was mostly quenched in methanol, where the monomer fluorescence was also very low. Further, excimer fluorescence was quenched in acidic condition and increased upon pH increase. Also, excimer emission was quenched upon heating without increasing back after cooling. That was probably caused by the temperature-induced unstacking and also by the aggregation of compounds.

Compound **Phen-Py-2** was more tending both to intramolecular stacking and aggregation. This compound lacked any significant responses upon eventual binding to ds-polynucleotides, both at acidic and neutral pH, except a small hypochromic change of the CD-spectra upon binding to *ct*-DNA. Opposite of **2**, more flexible **Phen-Py-1** with longer linker bound strongly, with micromolar and sub micromolar affinity, to all examined ds-polynucleotides. Quenching of excimer fluorescence upon addition of ds-polynucleotides combined with hypsochromic shift of emission maxima could be explained both by the dye unstacking and a partial intercalation of one aromatic unit between base pairs, or by unspecific binding of stacked dye along the polynucleotide backbone. In addition, CD measurements did not give unambiguous results since polynucleotide and dye absorbed UV light in the same wavelength region: small hypochromic change of *ct*-DNA spectra could be caused both by decrease in DNA helicity or by uniform orientation of dye concerning chiral axis. Finally, small decrease of CD spectra was observed in the pyrene absorption region that referred partial intercalation of aromatic moiety. Dye **Phen-Py-1** bound to dipeptidyl peptidase (DPPIII) enzyme mutant E451A with submicromolar affinity and showed interesting spectroscopic response: emission of excimer was totally quenched, but pyrene signal arose. This suggested important role of pyrene subunit, since pyrene had large hydrophobic surface that preferred binding to protein. Further, this result could lead to the development of new probes based on pyrene-phenanthridine chromophores that are able to switch fluorescence signals on/off upon binding to biomacromolecules.

Experimental section

Synthesis

Phenanthridine derivative of alanine amino acid (**Phen-AA**) has been prepared according to the procedure described earlier [13].

General procedure for the synthesis of the compounds Phen-Py-1 and Phen-Py-2:

To the solution of Boc-protected amino acid **Phen-AA** [13] in dichloromethane (4 mL) was added TFA-H_2O mixture (9:1, v/v; 2 mL) and the reaction was stirred at the room temperature overnight. Triflouroacetate salt of the deprotected amino acid was obtained as yellow oil after evaporation of the solvent. Deprotected compound was then dissolved in dry acetonitrile (3 mL) and appropriate pyrene-carboxylic acid, HBTU, HOBt and Et_3N were added. Reaction was stirred at the room temperature overnight. Products **Phen-Py-1** and **Phen-Py-2** were isolated by preparative thin layer chromatography in dichloromethane:methanol/9:1.

Phen-Py-1: **Phen-AA** (12.3 mg, 0.03 mmol), 1-pyrenebutyric acid (11.2 mg, 0.04 mmol), HBTU (11.4 mg, 0.03 mmol, 98%), HOBt (4.2 mg, 0.03 mmol, 97%) and Et_3N (16.8 µL, 0.12 mmol) were used according to the general procedure. **Phen-Py-1** was obtained as a white solid (9.4 mg, 56%).

M.p. = 131–132 °C; R_f = 0,8 (CH_2Cl_2:MeOH/9:1); IR (KBr) ν_{max}/cm^{-1}: 3418 (s), 3294 (s), 3038 (m), 2947 (m), 2858 (m), 1738 (s), 1643 (s), 1582 (m), 1535 (m), 1435 (m), 1377 (m), 1209 (m), 843 (s), 760 (s), 723 (m); ^{1}H NMR ($CDCl_3$) δ/ppm: 8.42 (d, J = 8.5 Hz, 1H, Phen), 8.31 (d, J = 8.1 Hz, 1H, Phen), 8.21–8.10 (m, 3H, Py), 8.07–7.93 (m, 6H, Phen, 5Py), 7.88 (d, J = 1.5 Hz, 1H, Phen), 7.73 (d, J = 7.8 Hz, 1H, Py), 7.66–7.45 (m, 3H, Phen), 5.98 (d, J = 7.7 Hz, 1H, NH), 5.12–5.03 (dd, J = 13.7, 6.0 Hz, 1H, CH), 3.75 (s, 3H, OCH_3), 3.48–3.39 (m, 1H, CH_2), 3.36–3.18 (m, 3H, CH_2) 2.92 (s, 3H, CH_3), 2.38–2.24 (m, 2H, CH_2), 2.22–2.09 (m, 2H, CH_2); ^{13}C NMR ($CDCl_3$) δ/ppm: 172.4 (C_q), 172.1 (C_q), 158.4 (C_q), 143.7 (C_q), 135.6 (C_q), 135.3 (C_q), 131.8 (CH-Ar), 131. 7 (C_q), 131.5 (C_q), 131.0 (C_q), 130.1 (C_q), 129.4 (CH-Ar), 128.8 (C_q), 128.7 (CH-Ar), 127.6 (CH-Ar), 127.5 (CH-Ar), 127.3 (CH-Ar), 126.9 (CH-Ar), 126.8 (CH-Ar), 126.5 (CH-Ar), 126.0 (CH-Ar), 125.0 (CH-Ar), 124.9 (CH-Ar), 124.9 (CH-Ar), 123.6 (C_q), 123.3 (CH-Ar), 122.9 (CH-Ar), 121.9 (CH-Ar), 53.2 (CH-Ala), 52.7 (OCH_3), 38.4 (CH_2), 36.1 (CH_2), 32.8 (CH_2), 27.3 (CH_2), 23.5 (CH_3); HRMS: *m/z*: calcd. for $C_{38}H_{32}N_2O_3^+$: 565.2485; found 565.2464 $[M+H]^+$.

Phen-Py-2: **Phen-AA** (12.0 mg, 0.03 mmol), 1-pyrenecarboxylic acid (9.2 mg, 0.04 mmol), HBTU (11.6 mg, 0.03 mmol, 98%), HOBt (4.2 mg, 0.03 mmol, 97%) and Et_3N (16.8 µL, 0.12 mmol) were used according to the general procedure. **Phen-Py-2** was obtained as a white solid (15.9 mg, 84%).

M.p. = 230–231 °C; R_f = 0.8 (CH_2Cl_2:MeOH/9:1); IR (KBr) ν_{max}/cm^{-1}: 3435 (s), 3261 (s), 1740 (m), 1634 (s), 1531 (m), 849 (m), 760 (m); ^{1}H NMR ($CDCl_3$) δ/ppm: 8.59 (d, J = 8.5 Hz, 1H, Phen), 8.51 (d, J = 7.3 Hz, 1H, Phen), 8.36 (d, J = 9.3 Hz, 1H, Py), 8.21 (d, J = 7.4 Hz, 1H, Py), 8.18–7.98 (m, 8H, 2Phen, 6Py), 7.91 (d, J = 9.3 Hz, 1H, Py), 7.78–7.67 (m, 2H, Phen), 7.66–7.58 (m, 1H, Phen), 6.66 (d, J = 7.6 Hz, 1H, NH), 5.51–5.40 (m, 1H, CH-Ala), 3.89 (s, 3H, OCH_3), 3.81–3.72 (m, 1H, CH_2-Ala), 3.57–3.47 (m, 1H, CH_2-Ala), 2.90 (s, 3H, CH_3); ^{13}C NMR ($CDCl_3$) δ/ppm: 172.1 (C_q), 169.5 (C_q), 158.7 (C_q), 135.6 (C_q), 133.1 (C_q), 132.1 (CH-Ar), 131.3 (C_q), 130.7 (C_q), 129.9 (CH-Ar), 129.4 (CH-Ar), 129.1 (CH-Ar), 129.1 (CH-Ar), 128.9 (CH-Ar), 127.4 (CH-Ar), 127.2 (CH-Ar), 126.7 (CH-Ar), 126.6 (CH-Ar), 126.1 (CH-Ar), 126.1 (CH-Ar), 124.6 (CH-Ar), 124.5 (CH-Ar), 124.2 (CH-Ar), 123.7 (C_q), 123.1 (CH-Ar), 122.1 (CH-Ar), 54.0 (CH-Ala), 52.9 (OCH_3), 38.5 (CH_2), 23.4 (CH_3); HRMS: *m/z*: calcd. for $C_{35}H_{26}N_2O_3^+$: 523.2022; found 523.2025 $[M+H]^+$.

Study of DNA/RNA interactions

General Procedures: The electronic absorption spectra of newly prepared compounds, UV-Vis titration and thermal melting experiments were measured on a Varian Cary 100 Bio spectrometer. Fluorescence spectra were recorded on Varian Cary Eclipse fluorimeter. CD spectra were recorded on JASCO J815 spectrophotometer. Fluorescence and CD spectra were recorded using appropriate 1 cm path quartz cuvettes; UV-Vis spectra were recorded in 1 cm path quartz cuvettes or using an immersion probe with 5 cm light path length. Polynucleotides were purchased as noted: calf thymus

(*ct*)-DNA, poly dAdT – poly dAdT, poly dGdC – poly dGdC and poly rA – poly rU (Sigma) and dissolved in sodium cacodylate buffer, I_c = 0.05 mol dm^{-3}, pH = 7.0. The calf thymus (*ct*-) DNA was additionally sonicated and filtered through a 0.45 μm filter [34]. Polynucleotide concentration was determined spectroscopically and expressed as the concentration of phosphates [34-35]. Mutant human DPP III was expressed and purified as described by Špoljarić et al. ili Recombinant human DPP III was obtained by heterologous expression in *Escherichia coli* and purification according to Špoljarić et al. [36-37]. Stock solutions of **Phen-Py-1-2** compounds were prepared by dissolving compounds in DMSO; total DMSO content was below 1% in UV-Vis and below 0.1 % in fluorimetric measurements. All measurements were performed in sodium cacodylate buffer, I_c = 0.05 mol dm^{-3}, **Phen-Py-1-2** concentrations below 3 × 10^{-6} mol dm^{-3} were used for UV-Vis absorbance measurement to avoid intermolecular association.

UV/Vis, CD, and fluorescence titrations: UV-Vis and fluorimetric titrations were performed by adding portions of polynucleotide solution into the solution of the studied compound. After mixing polynucleotides/protein with studied compounds it was observed that equilibrium was reached in less than 120 seconds. Compounds **Phen-Py-1** and **Phen-Py-2** showed decrease of their excimer fluorescence emission intensity upon time. Therefore, buffer solutions of compounds were prepared 24 hours before titration with polynucleotides to ensure stable spectra of compounds. In fluorimetric titrations, concentration of studied **Phen-Py-1-2** compounds were 2 × 10^{-6} mol dm^{-3}. Excitation wavelength of λ_{exc} = 352 nm was used for titrations to avoid absorption of excitation light caused by increasing absorbance of the polynucleotide or protein. Emission was collected in the range λ_{em}=350 – 650 nm. Fluorescence spectra were collected at r < 0.3 (r = [compound] / [polynucleotide]) to assure one dominant binding mode. Titration data were processed by means of Scatchard equation [29] and Global Fit procedure [31]. Calculations mostly gave values of ratio n = 0.2 ± 0.05, but for easier comparison all K_s values were re-calculated for fixed n = 0.2. Values for K_s have satisfactory correlation coefficients (> 0.98). In Scatchard equation values of stability constant (K_s) and ratio (n = [bound compound] / [polynucleotide]) are highly mutually dependent and similar quality of fitting calculated to experimental data is obtained for ± 20% variation for K_s and n; this variation can be considered as an estimation of the errors for the given binding constants. CD experiments were performed by adding portions of **Phen-Py-1-2** compound stock solution into the solution of polynucleotide ($c \approx$ 1-2×10^{-5} mol dm^{-3}). Examined **Phen-Py-1-2** compounds were chiral and therefore possessed intrinsic CD spectra. CD spectra were recorded with scanning speed of 200 nm/min. Buffer background was subtracted from each spectra, while each spectra was result of two accumulations.

Thermal melting experiments: Thermal melting curves for ds-DNA, ds-RNA and their complexes with studied compounds were determined by following the absorption change at 260 nm as a function of temperature. Absorbance scale was normalized. T_m values were the midpoints of the transition curves determined from the maximum of the first derivative and checked graphically by the tangent method. The ΔT_m values were calculated subtracting T_m of the free nucleic acid from T_m of the complex. Every ΔT_m value here reported was the average of at least two measurements. The error in ΔT_m is ± 0.5 °C.

Computational details

In order to sample the conformational flexibility of investigated systems and probe their intrinsic dynamics in the aqueous solution, classical molecular dynamics (MD) simulations were performed employing standard generalized AMBER force fields (ff14SB and GAFF) as implemented within the AMBER16 program package [38]. All structures were subsequently solvated in a truncated octahedral box of TIP3P water molecules spanning a 10 Å thick buffer of solvent molecules around each system, and submitted to periodic simulations where the excess positive charge was neutralized with an

equivalent number of chloride anions in monoprotonated systems corresponding to pH = 5. Upon gradual heating from 0 K, MD simulations were performed at 300 K for a period of 300 ns, maintaining the temperature constant using the Langevin thermostat with a collision frequency of 1 ps^{-1}. The obtained structures in the corresponding trajectories were clustered based on DBSCAN density-based algorithm according to recommended procedures. The idea behind this computational strategy was to investigate whether intrinsic dynamical features of studied conjugates both affect and can explain their tendency to undergo mutual association and form stacking interactions. The mentioned approach recently turned out as very useful in interpreting the affinities of several nucleobase – guanidiniocarbonyl-pyrrole conjugates towards single stranded RNA systems [13, 39].

To confirm that the described clustering analysis elucidated the most representative structures of each conjugate at both experimental pH values, we proceeded by calculating energies of the excited states responsible for the experimental UV/Vis spectra corresponding to isolated conjugates in the aqueous solution. For that purpose, we used the most abundant structure of each system in Figure 2 and performed the geometry optimization by the M06/6–31+G(d) model in the Gaussian 16 program package [40], with the water solvent effects modeled through the implicit SMD solvation. This was followed by the TD-DFT computations at the same level of theory considering 32 lowest singlet electronic excitations. The choice of this setup was prompted by its recent success in modeling UV/Vis spectra of organic and inorganic systems in various solvents [41–43].

Acknowledgment

Financial support from Croatian Science Foundation project **IP-2018-01-4694** and **IP-2020-02-8090** is gratefully acknowledged. Authors express their great appreciation to Dr. Ivo Piantanida for his valuable and constructive suggestions during the planning and development of this research work. Authors also extend their gratitude to Dr. Marija Abramić for her generous donation of dipeptidyl peptidase enzyme E451A.

References

[1] Radić Stojković, M.; Škugor, M.; Tomić, S.; Grabar, M.; Smrečki, V.; Dudek, Ł.; Grolik, J.; Eilmes, J.; Piantanida, I. *Org. Biomol. Chem.* **2013,** *11*, 4077-4085.

[2] Radić Stojković, M.; Škugor, M.; Dudek, Ł.; Grolik, J.; Eilmes, J.; Piantanida, I. *Beilstein J. Org. Chem.* **2014,** *10*, 2175-2185.

[3] Bains, G.; Patel, A. B.; Narayanaswami, V. *Molecules* **2011**, *16*, 7909-7935.

[4] Lakowicz, J. R., Introduction to Fluorescence. In *Principles of Fluorescence Spectroscopy*, Lakowicz, J. R., Ed. Springer US: Boston, MA, 1999; pp 1-23.

[5] Dukši, M.; Baretić, D.; Čaplar, V.; Piantanida, I. *Eur. J. Med. Chem.* **2010,** *45*, 2671-267

[6] Dukši, M.; Baretić, D.; Piantanida, I. *Acta Chim. Slov.* **2012,** *59*, 464-472.

[7] Radić Stojković, M.; Piotrowski, P.; Schmuck, C.; Piantanida, I. *Org. Biomol. Chem.* **2015,** *13*, 1629-1633.

[8] Hernandez-Folgado, L.; Schmuck, C.; Tomić, S.; Piantanida, I. *Bioorg. Med. Chem. Lett.* **2008,** *18*, 2977-2981.

[9] Orehovec, I.; Glavac, D.; Dokli, I.; Gredicak, M.; Piantanida, I. *Croat. Chem. Acta* **2017,** *90*, 603-611.

[10] Ban, Ž.; Matić, J.; Žinić, B.; Foller Füchtbauer, A.; Wilhelmsson, L. M.; Piantanida, I. *Molecules* **2020,** *25*, 2188.

[11] Matić, J.; Šupljika, F.; Tir, N.; Piotrowski, P.; Schmuck, C.; Abramić, M.; Piantanida, I.; Tomić, S. *RSC Adv.* **2016,** *6*, 83044-83052.

[12] Šmidlehner, T.; Badovinac, M.; Piantanida, I. *New J. Chem.* **2018,** *42*, 6655-6663.

[13] Matić, J.; Šupljika, F.; Tandarić, T.; Dukši, M.; Piotrowski, P.; Vianello, R.; Brozovic, A.; Piantanida, I.; Schmuck, C.; Stojković, M. R. *Int. J. Bio. Macromol.* **2019,** *134*, 422-434.

[14] Tumir, L.-M.; Piantanida, I.; Novak, P.; Žinić, M. *J. Phys. Org. Chem*. **2002,** *15*, 599-607.

[15] Jones, R. L.; Wilson, W. D. *Biopolymers* **1981,** *20*, 141-154.

[16] DeVoe, H.; Tinoco, I. *J. Mol. Biol.* **1962,** *4*, 518-527.

[17] Cantor, C. R. S. P. R. *Biophysical Chemistry Part. II*, W.H. Freeman: San Francisco, 1980; pp 399-404.

[18] Nogueira, J. J.; Plasser, F.; González, L. *Chem. Sci.* **2017,** *8*, 5682-5691.

[19] Browne, D. T.; Eisinger, J.; Leonard, N. J. *J. Am. Chem. Soc*. **1968,** *90*, 7302-7323.

[20] Leonard, N. J.; Cundall, R. L. *J. Am. Chem. Soc*. **1974,** *96*, 5904-5910.

[21] Mutai, K.; Gruber, B. A.; Leonard, N. J. *J. Am. Chem. Soc.* **1975**, *97*, 4095-4104.

[22] Chandross, E. A.; Dempster, C. *J. Am. Chem. Soc.* **1970**, *92*, 3586-3593.

[23] Albert, A.; Phillips, J. N. *J. Chem. Soc.* **1956**, 1294-1304.

[24] Singh, M. P.; Tarai, A.; Baruah, J. B. *ChemistrySelect* **2018,** *3*, 6364-6373.

[25] Bertocchi, M. J.; Zhang, X.-F.; Bajpai, A.; Moorthy, J. N.; Weiss, R. G. *J. Photochem. Photobiol. A: Chem.* **2018,** *355*, 467-478.

[26] Sorouraddin, M-H.; Amini, K.; Naseri, A.; Rashidi, M-R. *Open Chem.*, **2010**, *8*, 207-213.

[27] Saenger, W., Polymorphism of DNA versus Structural Conservatism of RNA: Classification of A-, B-, and Z-TYPe Double Helices. In *Principles of Nucleic Acid Structure*, Saenger, W., Ed. Springer New York: New York, NY, 1984; pp 220-241.

[28] Mergny, J. L.; Lacroix, L., *Oligonucleotides* **2003,** *13*, 515-537.

[29] McGhee, J. D.; von Hippel, P. H. *J. Mol. Biol.* **1974,** *86*, 469-489.

[30] Scatchard, G., *Ann. N. Y. Acad. Sci.,* **1949**, *51*, 660-672.

[31] Crnolatac, I.; Rogan, I.; Majić, B.; Tomić, S.; Deligeorgiev, T.; Horvat, G.; Makuc, D.; Plavec, J.; Pescitelli, G.; Piantanida, I., *Anal. Chim. Acta*, **2016,** *940*, 128-135.

[32]Lakowicz, J. R., Advanced Topics in Fluorescence Quenching. In *Principles of Fluorescence Spectroscopy*, Lakowicz, J. R., Ed. Springer US: Boston, MA, 1999; pp 267-289.

[33] Rodger, A.; Nordén, B., *Circular dichroism and linear dichroism*. Oxford University Press, USA: 1997; Chapter 2.

[34] Chaires, J. B.; Dattagupta, N.; Crothers, D. M. *Biochemistry* **1982,** *21*, 3933-3940.

[35] Chalikian, T. V.; Völker, J.; Plum, G. E.; Breslauer, K. J. *Proc. Natl. Acad. Sci. USA* **1999,** *96*, 7853-7858.

[36] Špoljarić, J.; Salopek-Sondi, B.; Makarević, J.; Vukelić, B.; Agić, D.; Šimaga, Š.; Jajčanin-Jozić, N.; Abramić, M. *Bioorg. Chem.* **2009,** *37*, 70-76.

[37] Špoljarić, J.; Tomić, A.; Vukelić, B.; Salopek-Sondi, B.; Agić, D.; Tomić, S.; Abramić, M. *Croat. Chem. Acta* **2011,** *84*, 259-268.

[38] Case, D. A.; Betz, R. M.; Cerutti, D. S.; Cheatham III, T. E.; Darden, T. A.; Duke, R. E.; Giese, T. J.; Gohlke, H.; Goetz, A. W.; Homeyer, N.; Izadi, S.; Janowski, P.; Kaus, J.; Kovalenko, A.; Lee, T. S.; LeGrand, S.; Li, P.; Lin, C.; Luchko, T.; Luo, R.; Madej, B.; Mermelstein, D.; Merz, K. M.; Monard, G.; Nguyen, H.; Nguyen, H. T.; Omelyan, I.; Onufriev, A.; Roe, D. R.; Roitberg, A.; Sagui, C.; Simmerling, C. L.; Botello-Smith, W. M.; Swails, J.; Walker, R. C.; Wang, J.; Wolf, R. M.; Wu, X.; Xiao, L.; Kollman, P. A. AMBER 2016, 2016, University of California, San Francisco.

[39] Ban, Ž.; Žinić, B.; Vianello, R.; Schmuck, C.; Piantanida, I. *Molecules* **2017**, *22*, 2213.

[40] Gaussian 16, Revision C.01, Frisch, M. J.; Trucks, G. W.; Schlegel, H. B.; Scuseria, G. E.; Robb, M. A.; Cheeseman, J. R.; Scalmani, G.; Barone, V.; Petersson, G. A.; Nakatsuji, H.; Li, X.; Caricato, M.; Marenich, A. V.; Bloino, J.; Janesko, B. G.; Gomperts, R.; Mennucci, B.; Hratchian, H. P.; Ortiz, J. V.; Izmaylov, A. F.; Sonnenberg, J. L.; Williams-Young, D.; Ding, F.; Lipparini, F.; Egidi, F.; Goings, J.; Peng, B.; Petrone, A.; Henderson, T.; Ranasinghe, D.; Zakrzewski, V. G.; Gao, J.; Rega, N.; Zheng, G.; Liang, W.; Hada, M.; Ehara, M.; Toyota, K.; Fukuda, R.; Hasegawa, J.; Ishida, M.; Nakajima, T.; Honda, Y.; Kitao, O.; Nakai, H.; Vreven, T.; Throssell, K.; Montgomery, J. A., Jr.; Peralta, J. E.; Ogliaro, F.; Bearpark, M. J.; Heyd, J. J.; Brothers, E. N.; Kudin, K. N.; Staroverov, V. N.; Keith, T. A.; Kobayashi, R.; Normand, J.; Raghavachari, K.; Rendell, A. P.; Burant, J. C.; Iyengar, S. S.; Tomasi, J.; Cossi, M.; Millam, J. M.; Klene, M.; Adamo, C.; Cammi, R.; Ochterski, J. W.; Martin, R. L.; Morokuma, K.; Farkas, O.; Foresman, J. B.; Fox, D. J. Gaussian, Inc., Wallingford CT, 2016.

[41] Pantalon Juraj, N.; Tandarić, T.; Tadić, V.; Perić, B.; Moreth, D.; Schatzschneider, U.; Brozović, A.; Vianello, R.; Kirin, S. I. *Dalton Trans.* **2022**, *51*, 17008–17021.

[42] Radović, M.; Hok, L.; Panić, M.; Cvjetko Bubalo, M.; Vianello, R.; Vinković, M.; Radojčić Redovniković, I. *Green Chem.* **2022**, *24*, 7661–7674.

[43] Boček, I.; Starčević, K.; Novak Jovanović, I.; Vianello, R.; Hranjec, M. *J. Mol. Liq.* **2021**, *342*, 117527.